KINETIC ANALYSIS OF CRACK FORMATION IN CATHODIC ELECTRODEPOSITED COATINGS: INFLUENCE OF POLYMERIZATION TIME AND THERMAL CONDITIONS

DAMIAN PETI[1], PATRIK FEJKO[1], ROBERT ROPOVIK[1], RADOSLAV VANDZURA[1], MIROSLAV GOMBAR[2], JOZEF DOBRANSKY[1]

[1]Technical University of Kosice, Faculty of Manufacturing Technologies with a seat in Presov, Presov, Slovak Republic

[2]University of West Bohemia Pilsen, Faculty of Mechanical Engineering, Plzen, Czech Republic

DOI: 10.17973/MMSJ.2025_06_2025048

damian.peti@tuke.sk

This study investigates the influence of material properties and processing conditions on the crack length of electrophoretic coatings on cold-rolled low-carbon steel. The selected steel, identified by VDA239-100 CR4 and CR5 and DIN EN 10130 DC05 and DC06 standards, features a low carbon and titanium content, offering improved plasticity and mechanical properties. The bending test, conducted according to ISO 6860:2006 on a conical mandrel, was employed to evaluate the flexibility and mechanical integrity of the coating under controlled deformation. Statistical analyses of model adequacy, using the coefficient of determination (R^2), indicate that the model explains approximately 70.31% of the variability in crack length. The study also demonstrates the application of the Design of Experiments (DOE) methodology to assess the influence of polymerization time and thermal conditions on crack formation. Graphical analysis reveals the significant effects of polymerization duration and temperature, as well as phosphating time, on the crack length, with the findings providing a deeper understanding of the factors contributing to coating behavior.

KEYWORDS

Cataphoresis, Electrophoretic coatings, Design of Experiments, Crack length, Microscopic Analysis

1 INTRODUCTION

Electrophoretic coatings, commonly referred to as electrocoat or electropaint, constitute a class of organic coatings dispersed in an aqueous medium, characterized by the presence of an electric charge [Fejko 2024]. This charge enables deposition onto a metallic substrate of opposite polarity under the influence of an applied electric field [Brüggemann 2020]. Following deposition, the coating undergoes an irreversible transition to a water-insoluble state, and subsequent curing at temperatures ranging from 100 to 200 °C results in the formation of highly durable and mechanically robust protective films [Almeida 2003].

The introduction of electrodeposition coatings (E-coats) in the 1960s represented a transformative advancement in corrosion protection for automotive components [Akafuah 2016]. At present, E-coating remains the predominant coating method in the automotive industry, offering superior corrosion resistance and mechanical durability [Besra 2007].

Ensuring effective corrosion protection is paramount for extending the longevity of coated surfaces. One of the most advanced techniques employed for this purpose is cataphoretic deposition which facilitates the uniform application of protective layers [Rossi 2006]. This method is particularly distinguished by its ability to achieve strong adhesion and consistent film distribution, even on substrates with complex geometries, thereby ensuring comprehensive surface coverage and long-term durability [Romano 2005]. The effectiveness of the anti-corrosion performance of paint coatings is determined by the synergistic interaction of anti-corrosion pigments, the coating's barrier properties, and its adhesion to the substrate [Goeke 2014]. Proper surface preparation prior to coating application represents a critical and complex stage in corrosion protection technologies [Trzepiecinski 2023]. Steel surfaces are often contaminated by various substances, including reaction products formed through environmental exposure (such as scale and rust), as well as organic residues from oils, and greases [Sternadelova 2023]. Additionally, atmospheric pollutants, such as dust and water-soluble salts—often imperceptible to the human eye—can accumulate on the surface. Their effective removal typically necessitates a sequence of preparatory treatments to ensure optimal coating performance [Grzesik 2016], [Skotnicki 2021].

The influence of deposition parameters on coating properties has been extensively studied. Rossi et al. [Rossi 2017] investigated the optimization of the deposition process and the properties of cataphoretic coatings applied to aluminum foam substrates. Their findings demonstrated a significant impact of the coating on the corrosion resistance of the foam, evaluated through acetic acid salt spray testing and electrochemical impedance spectroscopy. The incorporation of a dye into the resin enabled the identification of three distinct cell types: black-colored cells corresponding to coated regions, light-colored cells indicating uncoated areas, and purple-colored cells representing partial resin coverage. The study underscored the challenge of achieving uniform coating distribution across complex aluminum foam structures. Furthermore, deposition voltage was identified as a critical parameter directly influencing the resulting coating thickness.

Zanella et al. [Zanella 2014] conducted a study examining the relationship between the electrochemical characteristics of metal substrates and the performance of electrophoretic clear coatings. Their investigation focused on three distinct substrate types: active (bare steel), passive (nickel), and noble (gold), with the objective of determining the extent to which the substrate's electrochemical behavior influences key coating properties, including barrier performance, adhesion, and water absorption. The results confirmed that the functional attributes of the coating are significantly affected by the substrate type and its electrochemical activity [Calovi 2021].

Subsequent investigations by Almeida et al. [Almeida 2003] and Deflorian et al. [Deflorian 2006] established a direct correlation between the applied deposition voltage and the resulting coating thickness, demonstrating that higher voltages yield thicker layers. Cataphoretic deposition remains a promising technique for surface coating applications due to its precise control over film formation. By adjusting the deposition voltage, thinner coatings can be achieved at lower voltages, whereas excessive voltage levels must be avoided, as they can lead to defect formation, such as bubble generation, which compromises the coating's integrity and performance.

Beyond the fundamental deposition parameters, post-deposition processing conditions, specifically polymerization time and thermal treatment, exert a critical influence on the mechanical integrity and long-term stability of electrophoretic coatings [Krasinskyi 2021]. Empirical investigations have substantiated that crack initiation and propagation within these coatings, particularly on low-carbon steel substrates, are governed by a complex interplay between material characteristics and process variables. The kinetics of crack evolution are intrinsically linked to the thermal and polymerization regimes, where insufficient curing can result in suboptimal adhesion and premature mechanical failure, while excessive thermal exposure may induce residual stresses, leading to structural degradation.

Previous research [Peti 2024] conducted on the same material utilized non-destructive testing methods to evaluate the effect of degreasing conditions on the thickness and structural integrity of the electrophoretic coating. These studies involved thickness measurements and structural observations, providing valuable insights into how pre-treatment parameters influence the final layer formation. The findings confirmed that optimizing pre-treatment conditions is crucial for achieving a uniform and functionally effective coating, ensuring proper adhesion and minimizing structural irregularities. However, while non-destructive measurements provided essential information regarding layer uniformity and morphology, they do not fully capture the mechanical properties and failure mechanisms of the coating under stress conditions. To comprehensively assess the integrity of the electrophoretic layer, it is necessary to conduct destructive testing, focusing on crack formation, propagation, and the impact of polymerization time and thermal conditions on these phenomena.

2 MATERIAL AND METHODS

The selection of polymerization parameters was based on real-time parameters used in the industrial cathodic electrodeposition (CED) line at KTL, s.r.o. Prešov, ensuring the study's findings are directly applicable to industrial practice. The process conditions replicate typical curing cycles, optimizing coating mechanical and corrosion resistance properties. These parameters were refined through pilot experiments to optimize process variables such as voltage, polymerization temperatures, and phosphating times, ensuring process efficiency and quality control. To ensure efficiency in terms of cost and time while maintaining reliability, it was essential to minimize the number of trials. The Design of Experiments (DoE) methodology was applied, enabling the acquisition of the maximum amount of relevant information with high statistical accuracy and numerical reliability. This scientifically validated approach allowed for optimal experimental design while preserving objectivity. The study used a Central Composite Design (CCD) to model nonlinear relationships and capture parameter interactions efficiently, minimizing experimental runs. By analyzing factors such as deposition time, varnishing voltage, and polymerization time, the CCD approach facilitated the development of a nonlinear model that accurately describes the interactions between these key process parameters.

2.1 *Material selection – VDA 239-100 CR4*

This study investigates the selection of steel types VDA239-100 CR4, CR5, and DIN EN 10130 DC05, DC06, focusing on their widespread use in industries such as automotive manufacturing, where high formability and surface quality are essential for coating processes like cathodic electrodeposition (CED). The chosen materials are characterized by their compliance with internationally recognized standards (VDA 239-100 and DIN EN 10130), ensuring their suitability for forming and surface treatment applications.

Properties	Value
Yield point Rp 0,2 [Mpa]	140-180
Tensile strength Rm [Mpa]	270-350
Hardness by Brinell HBW	267
Elongation (A_{80})	≥ 39 %
r – Value r(90/20)	≥ 1.9
r – Value m/20	≥ 1.6
n - Value (n_{10-20}/Ag)	≥ 0.20

Table 1. Mechanical properties of mild steel acc. VDA 239-100 CR4

The low-carbon steels selected in this study exhibit excellent formability, high surface quality, and good adhesion properties, which are critical for evaluating the effects of phosphating and CED on crack formation. Their mechanical properties align with prior research on the behavior of coatings under thermal and mechanical stresses, providing a solid foundation for investigating the durability of electrodeposited coatings.

The material selection is particularly relevant to the investigated process, as these steels are widely used in applications requiring corrosion protection and enhanced coating adhesion. Their interaction with phosphating and CED coatings makes them ideal substrates for analyzing crack formation mechanisms under varying polymerization conditions.

2.2 *Methodology of Production Processes*

The experiment was conducted on an automated cataphoresis production line (KTL) to replicate industrial conditions. The study was carried out on a total of 88 specimens, adhering to standardized methodological protocols to maintain consistency and reproducibility of the results. To ensure optimal surface properties and adhesion, the samples underwent a sequence of technological pre-treatment processes prior to coating application. The variation in process parameters, including polymerization time, temperature, and phosphating conditions, was based on a Central Composite Design (CCD), enabling the systematic evaluation of their combined influence on crack formation in cathodic electrodeposited coatings:

1. Chemical Degreasing

Surface contaminants were removed through degreasing, with key variables including chemical concentration [DEGR_{con}] (PRAGOLD 57N - degreasing agent is a highly alkaline, low-foaming solution with moderate emulsifying properties), temperature [°C], and duration ([DEGR_{time}]=3/6/8/10/13 min) based on the experimental design methodology (DoE). This step was essential for ensuring proper coating adhesion.

2. Zinc-Phosphate Coating

Phosphating was carried out using a standard chemical composition, with immersion times of 3 and 7 minutes. The phosphate bath temperature (50/60 °C) was maintained as a constant parameter.

3. Cataphoretic Deposition

The coating was applied in an immersion bath under controlled conditions, with paint composition (solids content) kept constant. Voltage levels ([KTL_U]=200V/250V/300V) and deposition time were adjusted according to DoE to evaluate electrical parameter effects.

4. Polymerization process

Curing was performed with polymerization temperature ([DEGR_{temp}]= 40/80°C) regulated in a furnace. Polymerization time was varied to analyze its influence on coating integrity.

2.3 *Bending Test on a Conical Mandel*

The bending test (Figure 1.) was conducted utilizing the Gamin TQC SP 1831 apparatus to assess the flexibility and mechanical integrity of surface coatings applied to metallic substrates. This evaluation determines the resistance of the coating to mechanical stress and potential crack propagation when subjected to controlled deformation. The experiment adheres strictly to the ISO 6860:2006 standard, titled "Paints and Varnishes – Bending Test (on a Conical Mandrel)."

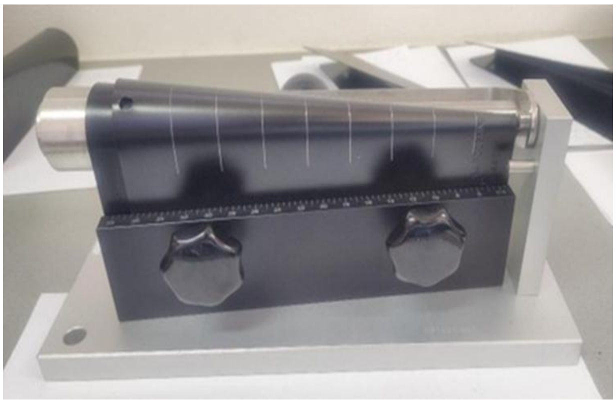

Figure 1. Bending Test on a Conical Mandel

The test was performed under controlled laboratory conditions at a stable temperature of 23 °C to minimize external influences on the material response. The conical mandrel, with a diameter range of 3.1 mm to 38 mm, enabled a gradual deformation of the test panel, allowing for an evaluation of the coating's elastic and adhesion properties. The bending procedure involved a single, continuous 180° movement, executed within a strictly defined time frame of 2 to 3 seconds, ensuring reproducibility and consistency of results.

3 RESULTS AND DISCUSSION

3.1 *Statistical Analysis of Model Adequacy and Crack Length Variability*

Tab. 2 presents the evaluation of model adequacy and the impact of various factors on the crack length of the formed coating layer. The coefficient of determination (R^2), which quantifies the variability in crack length, is approximately 75%, indicating a strong correlation between the model and the observed data. The adjusted statistical metrics in Table 1 provide an assessment of the model's ability to describe the relationship between the controlled chemical and physical input factors and the resulting system response, as measured by the crack length of the KTL coating layer. The analysis demonstrates that 70.31% of the total variability in crack length is accounted for by the model, supporting its reliability in predicting the coating's behavior under experimental conditions. Furthermore, the mean crack length observed for the electrophoretic layer is 70.17 mm, offering a quantitative benchmark for assessing the integrity of the coated system.

Source	Value
RSquare	0.754413
RSquare Adj	0.703096
Root Mean Square Error	17.33732
Mean of Response	70.16756
Observations (or Sum Wgts)	82

Table 2. Summary of Model Adequacy Evaluation Based on Statistical Analyses

According to Tab. 3, it can be concluded that the variability caused by random error is significantly lower than the measurement variability explained by the model. The p-values (Prob > F) indicate the adequacy of the applied model based on the Fisher-Snedecor test. The chosen significance level (α = 0.05) serves as the threshold for determining the statistical significance of the model, confirming its validity in describing the relationship between the studied parameters.

Source	DF	Sum of Squares	Mean Square	F Ratio	p
Model	14	61864.52	4418.89	14.7011	<0.0001
Error	67	20139.03	300.58	-	-
C	81	82003.56	-	-	-

Table 3. ANOVA – Analysis of Variance

Based on the lack-of-fit errors presented in Tab. 4, it can be stated that the significance level of 1.8192 allows for the acceptance of the null statistical hypothesis at the chosen significance level (α = 0.05). This indicates that the residual variance is less than or equal to the within-group variance, thereby confirming that the model is adequate and statistically valid for describing the observed system.

Source	DF	Sum of Squares	Mean Square	F Ratio	p
Lack of Fit	66	19972.69	302.616	1.8192	0.5389
Pure Error	1	166.349	166.349	-	-
Total Error	81	20139.03	-	-	-

Table 4. Lack of Fit

3.2 *Graphical Analysis of the Influence of Polymerization Time and Thermal Conditions*

The formation and propagation of cracks in cathodic electrodeposited coatings are strongly influenced by post-deposition processing conditions, particularly polymerization time and thermal exposure. The curing process plays a decisive role in determining the mechanical integrity of the coating, as it affects the crosslinking density, adhesion properties, and residual stress distribution within the film. Insufficient polymerization may result in weak adhesion and premature crack initiation, whereas excessive thermal exposure can lead to internal stresses, ultimately contributing to crack propagation and structural degradation. To comprehensively evaluate these effects, a series of experimental trials were conducted based on a structured Design of Experiments (DOE) approach. This methodology enabled the systematic assessment of key processing parameters and their impact on crack formation. The experimental data were analyzed using graphical tools, providing a visual representation of the relationship between polymerization duration, thermal conditions, and crack length.

The graphical analysis presented in Figures 2, 3, 4, and 5 illustrates the trends observed during destructive testing, offering insight into the kinetic behavior of crack formation. By identifying critical thresholds in polymerization time and thermal exposure, this analysis contributes to optimizing process parameters to enhance coating performance and durability.

Figure 2. illustrates the relationship between polymerization duration, temperature, and crack length, revealing significant variations in mechanical response under different processing conditions. The data suggest that polymerization time and temperature exhibit a complex, nonlinear influence on crack formation, with distinct trends emerging at different experimental levels.

At the minimum experimental conditions, substantial variations in crack length are observed. When polymerization is set at 13 minutes, the crack length reaches 53.98 mm. Extending the polymerization time to 27 minutes results in a reduction to 26.15 mm, indicating an improvement in coating integrity. The lowest recorded crack length, 24.59 mm, corresponds to a polymerization temperature of 150 °C, suggesting that moderate curing temperatures contribute to enhanced mechanical stability. A notable trend is the initial increase in crack length with polymerization time, peaking at 42.71 mm at 20 minutes. Beyond this threshold, an extended polymerization duration reduces crack formation, with a final measurement of 30.25 mm at 27 minutes. This decrease of 5.66 mm compared to the initial 13-minute condition suggests that prolonged polymerization enhances crosslinking density and reduces internal stresses, mitigating crack propagation. In contrast, the influence of higher polymerization temperatures—particularly at 250 °C—is more pronounced. At 13 minutes, the crack length is measured at 78.57 mm, indicating significant thermal stress within the coating. The crack length reaches a maximum of 84.71 mm at 17 minutes, highlighting an adverse effect of excessive heat exposure at shorter polymerization times. However, further extending polymerization duration leads to a decline in crack length, reaching 56.40 mm at 27 minutes. This reduction suggests that prolonged polymerization time at elevated temperatures allows for stress relaxation and improved structural integrity of the coating.

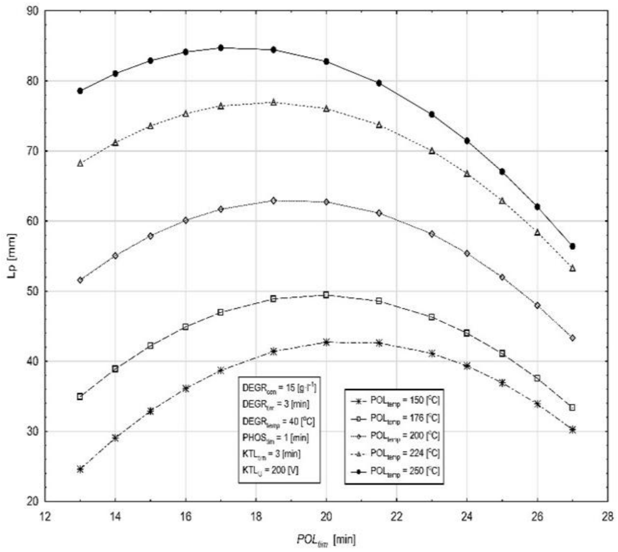

.

Figure 2. The influence of polymerization time and polymerization temperature on the variation of the formed layer under minimum conditions of the Design of Experiments Methodology

Under maximum experimental conditions shown in Figure 3., the variations in crack length follow a distinct pattern, influenced by both polymerization duration and temperature. The observed difference between the maximum and minimum crack lengths across varying polymerization times is 5.82 mm, indicating a significant effect of processing conditions on the mechanical integrity of the electrophoretic coating.

At a polymerization temperature of 176 °C and a duration of 13 minutes, the minimum crack length of 74.08 mm is recorded, highlighting the potential for moderate curing temperatures to reduce defect formation. However, as polymerization time increases, the crack length also increases, reaching a peak of 82.38 mm at approximately 17.28 minutes. Beyond this threshold, further polymerization leads to a gradual decline in crack length, suggesting that prolonged exposure at this temperature facilitates improved stress distribution and structural stability. A polymerization temperature of 150 °C yields the lowest crack length of 54.08 mm at 27 minutes, reinforcing the trend that extended polymerization under controlled thermal conditions enhances coating performance. Conversely, excessive thermal exposure at 224 °C results in the maximum crack length of 84.24 mm at 13 minutes. The crack length continues to rise with increasing polymerization time, peaking at 96.89 mm at approximately 17.35 minutes. Thereafter, a reduction to 87.73 mm at 27 minutes is observed, suggesting that prolonged polymerization time mitigates the adverse effects of high-temperature curing. At the extreme polymerization temperature of 250 °C, crack length continues to increase up to a deposition time of 20 minutes, reaching a maximum of 100.19 mm. This observation indicates that excessive thermal exposure during the initial stages of polymerization exacerbates crack formation due to increased internal stresses. However, as polymerization time progresses beyond 20 minutes, a subsequent decline in crack length is observed, suggesting that prolonged curing under high-temperature conditions enables partial stress relaxation and improved coating cohesion.

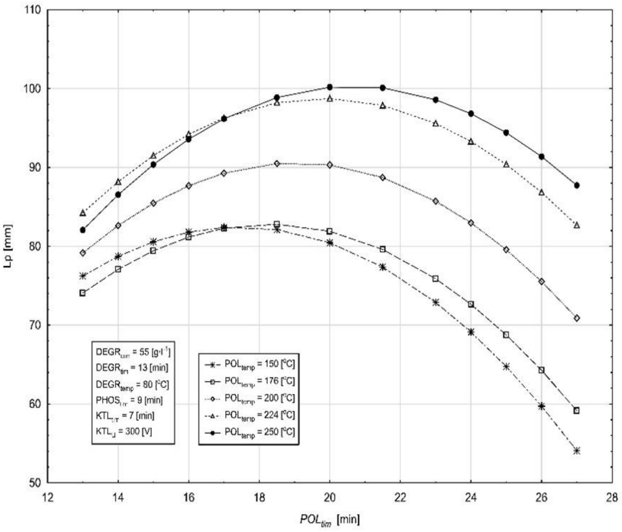

Figure 3. The influence of polymerization time and polymerization temperature on the variation of the formed layer under maximum conditions of the Design of Experiments Methodology

Figure 4. illustrates the combined influence of polymerization and phosphating times on crack length formation, emphasizing their interactive effect on coating integrity. The data reveal a complex relationship in which variations in both parameters significantly impact crack propagation.

At the minimum factor levels, the shortest crack length of 24.59 mm is observed for a phosphating time of 1 minute and a polymerization time of 13 minutes. As polymerization time increases, crack length initially follows an increasing trend, reaching a peak of 42.71 mm at 20 minutes. Notably, at this polymerization duration, a phosphating time of 9 minutes intersects with the curve, demonstrating minimal crack lengths as polymerization progresses. With further polymerization, crack length reduces to 16.33 mm at 27 minutes, indicating that extended polymerization, in combination with adequate phosphating, contributes to improved coating stability and reduced crack formation. Conversely, when polymerization is maintained at 13 minutes, the maximum crack length of 40.42 mm occurs at a phosphating time of 7 minutes. Beyond this, crack length continues to increase, reaching a peak value of 47.89 mm at approximately 16.38 minutes. This point marks the intersection with the curve representing a phosphating time of 5 minutes, suggesting that an insufficiently long phosphating stage may exacerbate crack formation. The interaction of these parameters leads to a transition toward maximal crack lengths, culminating at 50.08 mm at a polymerization time of 20 minutes. Beyond this peak, crack length exhibits a declining trend, decreasing to 43.92 mm at approximately 23.51 minutes, where the phosphating time of 3 minutes intersects with the curve. The 3-minute phosphating time itself reaches a maximum crack length of 32.16 mm at 27 minutes, indicating that shorter phosphating times may result in less effective surface preparation, thereby influencing crack formation dynamics.

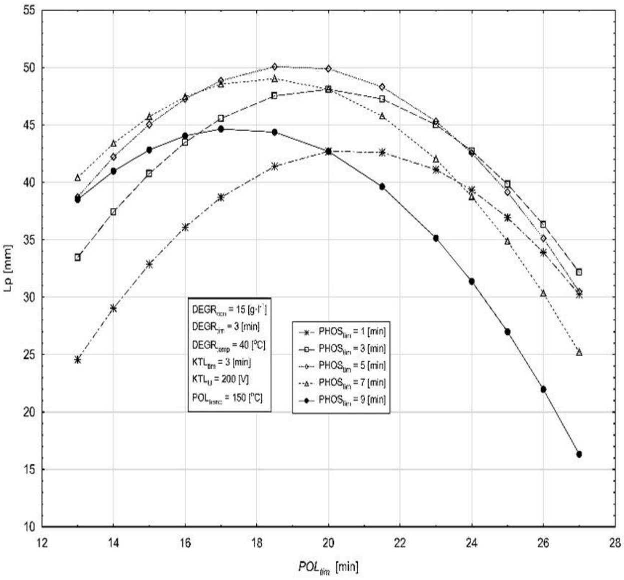

Figure 4. The influence of polymerization time and phosphating time on the variation of the formed layer under minimum conditions of the Design of Experiments Methodology

Figure 5 presents the influence of polymerization and phosphating times on crack length formation under maximum factor levels, highlighting their combined effect on coating performance. The data indicate that both parameters significantly influence crack propagation, with distinct trends emerging as polymerization and phosphating times vary.

At the maximum factor levels, the shortest crack length of 82.07 mm is observed for a phosphating time of 9 minutes and a polymerization time of 13 minutes. As polymerization progresses, crack length increases, reaching a peak of 100.19 mm at 20 minutes. At this point, the curve intersects with the trend corresponding to a phosphating time of 1 minute, suggesting that inadequate phosphating may contribute to increased crack formation. Beyond this peak, crack length decreases, reaching 73.82 mm at 27 minutes, indicating that prolonged polymerization can mitigate crack propagation when paired with sufficient phosphating treatment.

For a polymerization time of 13 minutes, the maximum crack length of 97.91 mm is observed at a phosphating time of 3 minutes. With increasing polymerization duration, crack length rises, reaching approximately 105.28 mm at 16.38 minutes, where it intersects with the curve representing a phosphating time of 5 minutes. This phosphating time continues to contribute to crack propagation, culminating in a maximum crack length of 107.57 mm at 18.5 minutes. However, beyond this critical threshold, crack length exhibits a declining trend, decreasing to 101.33 mm at approximately 23.33 minutes, where the curve for a phosphating time of 7 minutes intersects. The phosphating time of 7 minutes results in a crack length of 89.65 mm at 27 minutes, reinforcing the observation that extended phosphating durations contribute to enhanced coating integrity and reduced crack formation. The data suggest that while increased polymerization time generally leads to reduced crack propagation, phosphating duration plays a crucial role in defining the mechanical stability of the coating. Optimal phosphating times appear to mitigate the negative effects of prolonged polymerization, highlighting the necessity of precise process control to achieve coatings with superior adhesion and durability.

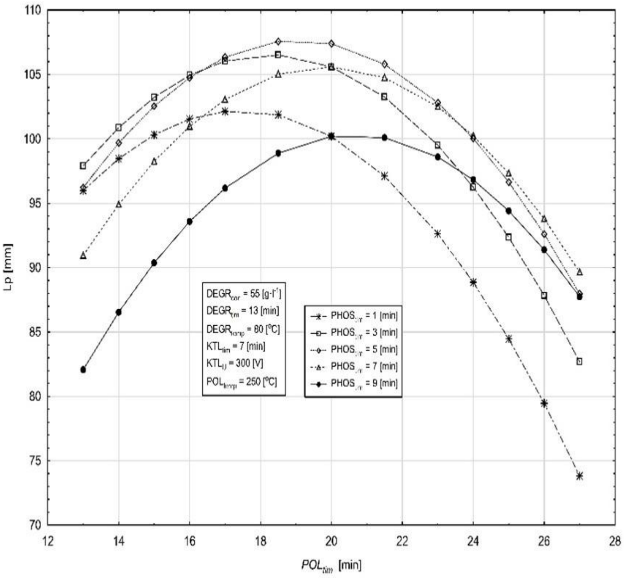

Figure 5. The influence of polymerization time and phosphating time on the variation of the formed layer under maximum conditions of the Design of Experiments Methodology

3.3 *Microscopic Analysis of Crack Morphology*

The microscopic evaluation of crack morphology was performed utilizing the Keyence Polarize microscope, a high-precision optical instrument designed for detailed surface analysis. This microscope provides advanced imaging capabilities, including high-resolution magnification and polarization features that enhance contrast and minimize glare on reflective surfaces. These attributes are particularly beneficial for the structural assessment of electrophoretic coatings, allowing for a clearer distinction of microstructural features and crack propagation patterns. The non-contact measurement system further ensures that the integrity of delicate surface structures remains unaffected, preserving the accuracy and reliability of the observed data.

Figures 6 and Figure 7 depict the microscopic analysis, revealing significant variations in crack morphology as a function of polymerization parameters. These variations in crack propagation, width, and depth correlate directly with macroscopic crack length measurements and coating integrity.

The microscopic data provide valuable insights into the microstructural behavior of electrophoretic coatings, highlighting the critical role of process parameters such as polymerization time and thermal conditions (see Table 5) in determining their mechanical performance and susceptibility to defects.

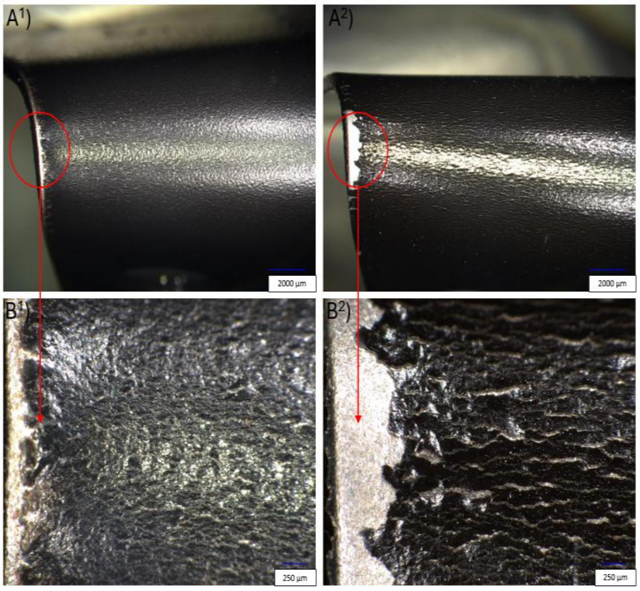

Figure 6. Microscopic Analysis of Crack Morphology Under Minimum (A^1, B^1) and Maximum (A^2, B^2) Experimental Conditions of Design of Experiments Methodology – Keyence Polarize 20x, 100x Magnification

The first set of microscopic images in Figure 6 (A^1, B^1 and A^2, B^2), captured at 20× and 100× magnifications, offers a broader view of crack propagation and coating integrity. The lower magnification images (A^1, A^2) reveal the overall distribution of cracks under varying polymerization conditions, with visible differences in crack density and spread. The higher magnification images (B^1, B^2) provide detailed insights into crack formation mechanisms, surface irregularities, and defect density. These observations directly correspond to the macroscopic measurements of crack length, indicating that increased polymerization times generally lead to longer cracks, especially under higher thermal conditions.

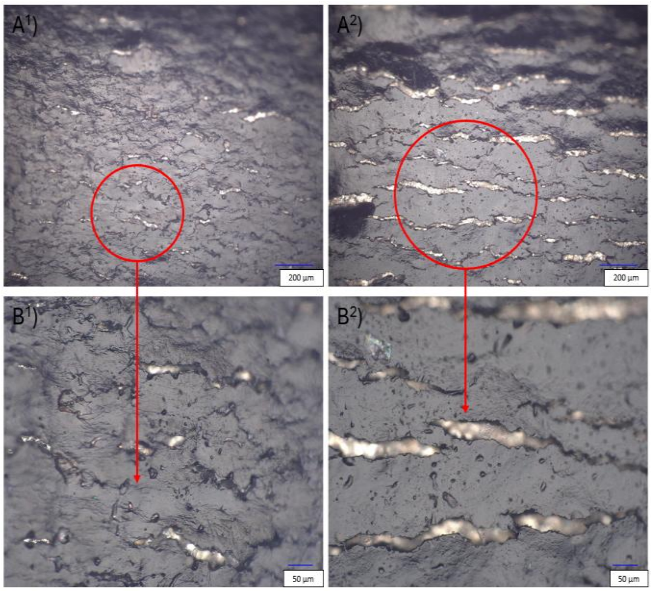

Figure 7. Microscopic Analysis of Crack Morphology Under Minimum (A^1, B^1) and Maximum (A^2, B^2) Experimental Conditions of Design of Experiments Methodology - Keyence Polarize 300x, 500x Magnification

The second set of images in Figure 7, captured at 300× and 500× magnifications, offers an even more detailed examination of microstructural defects within the electrophoretic coating. These high-resolution images allow for precise identification of crack propagation patterns and coating cohesion.

Under minimum experimental conditions (A^1, B^1):

- The images exhibit irregular crack patterns with broader spacing, corresponding to shorter macroscopic crack lengths measured (24.59 mm).
- These defects are attributed to insufficient polymerization and suboptimal thermal energy, which result in reduced cohesion and poor uniformity in the coating layer, as evidenced by the larger, more irregular cracks.

Under maximum experimental conditions (A^2, B^2):

- The coating appears more uniform, with fewer but longer cracks, correlating with increased macroscopic crack length (up to 42.71 mm).
- Higher polymerization times and elevated temperatures improve coating uniformity but also promote thermal stress-induced crack propagation, leading to increased crack length despite improved coating cohesion, as seen in both microscopic and macroscopic data.

The observed crack patterns in both microscopic and macroscopic analyses align with existing studies on electrophoretic coatings. Specifically, these findings confirm that:

- Suboptimal curing conditions lead to weaker cross-linking of the polymer matrix, reducing coating integrity and resulting in shorter and more irregular cracks.
- Excessive thermal exposure promotes internal stress accumulation within the coating, causing shrinkage-induced cracking and increasing crack length despite improved adhesion and coating uniformity.

These correlations between microscopic crack morphology and macroscopic crack length measurements emphasize the importance of optimal polymerization and thermal conditions in ensuring the mechanical performance and overall integrity of electrophoretic coatings.

Experimental Conditions of samples	
Polymerization	**Value**
Deposition Time [min]	17/23
Temperature [°C]	176/224
Phosphating	**Value**
Deposition Time [min]	3/7
Cataphoresis	**Value**
Deposition Time [min]	4/5
Voltage [V]	226/274

Table 5. Minimum and Maximum Experimental Conditions of samples (A, B) of Microscopic Analysis of Crack Morphology

3.4 *Statistical Validation of Crack Formation*

To quantify crack characteristics, statistical modeling was applied. The results indicate:

- The results revealed a strong correlation between processing parameters and crack length, with an R^2 value of 0.754 and an adjusted R^2 value of 0.703. The

R² value indicates that approximately 75% of the variability in crack length is explained by the model, highlighting a robust relationship between the processing parameters and crack formation. However, the slightly lower adjusted R² value accounts for the number of predictors in the model and penalizes the inclusion of variables that do not significantly contribute to explaining the response. This adjustment suggests that while the model explains a substantial portion of the variability, some predictors might not be meaningfully enhancing the model's explanatory power.

- The difference between R² and adjusted R² emphasizes the potential presence of non-significant predictors in the model. Although these predictors are included, their contribution to explaining the crack length variability may be limited. The adjusted R² value provides a more conservative estimate by accounting for the effect of including unnecessary predictors, indicating that further refinement of the model may be needed to optimize the predictor set and improve the overall explanatory power.
- The model explains 70.31% of the observed variability, as validated by ANOVA results ($p < 0.0001$), confirming its predictive reliability.
- The p-value of the lack-of-fit test (0.5389) indicates that the null hypothesis, which states that the model fits the data adequately, cannot be rejected at the 5% significance level. A lower p-value (e.g., <0.01) would suggest a significant lack of fit, meaning the model does not adequately describe the data. However, in this case, the relatively high p-value confirms that there is no significant lack of fit, implying that the model sufficiently represents the observed system without the need for additional complexity or modifications. This conclusion is further supported by the fact that the residual variance remains within an acceptable range compared to the within-group variance.

4 DISCUSSION AND IMPLICATIONS

The findings of this study provide a comprehensive understanding of the relationship between processing parameters, coating structure, and mechanical performance in electrophoretic coatings. By integrating microscopic analysis, statistical modeling, and prior non-destructive evaluations of coating thickness, a deeper insight into crack formation mechanisms and structural stability has been established.

- Process-Structure-Performance Relationship

Experimental results confirm that polymerization time, curing temperature and phosphating significantly influence the mechanical stability of the electrophoretic coating. These factors directly impact the degree of polymer cross-linking, which affects adhesion strength and crack resistance.

Previous research based on non-destructive thickness measurements such as The effect of degreasing temperature on the thickness of the formed layer created by cataphoretic painting [Peti 2024] demonstrated that pre-treatment conditions, such as degreasing temperature and chemical concentration, influence coating uniformity and adhesion. It was established that improper pre-treatment can lead to irregular layer formation, which ultimately affects the structural integrity of the coating.

The statistical model supports these conclusions, with an R² value of 0.754 and an adjusted R² of 0.703, demonstrating a strong correlation between experimental parameters and crack length. The model explains 70.31% of the observed variability, further validated by ANOVA results ($p < 0.0001$), confirming the predictive capacity of the approach.

- Thermal Effects and Crack Propagation

A key observation in this study is the transient increase in crack length under maximum experimental conditions, attributed to initial thermal stress accumulation during polymerization. This aligns with prior thickness evaluations, which showed that variations in pre-treatment conditions impact deposition characteristics, ultimately influencing the cross-linking density of the polymer structure.

While thermal exposure initially promotes crack formation, prolonged polymerization induces a stabilization effect, where the coating structure adjusts and compensates for initial stress concentrations. The data suggest that beyond a certain curing threshold, stress relaxation mechanisms within the polymer matrix reduce defect formation, improving overall mechanical performance.

- Correlation Between Microscopic and Macroscopic Observations

The combination of high-resolution microscopic imaging and macroscopic crack length analysis provides a comprehensive multi-scale evaluation of coating failure mechanisms. The consistency between microstructural defects and observed crack propagation confirms that structural irregularities at the microscopic level are strongly correlated with macroscopic mechanical failure.

These observations align with previous non-destructive thickness measurements, reinforcing the necessity of an integrated evaluation framework that accounts for both coating formation and long-term mechanical behavior. The convergence of experimental data across different analytical scales validates the Design of Experiments (DOE) methodology as an effective tool for industrial coating process optimization.

- Optimal conditions on minimizing cracks

The optimal conditions for minimizing cracks in electrophoretic coatings were identified as a polymerization temperature of 150°C, a polymerization time of 27 minutes, and a phosphating time of 9 minutes. The data shows that at moderate temperatures (150°C) and a polymerization duration of 27 minutes, the crack length is minimized (24.59 mm), indicating optimal crosslinking and reduced residual stresses. Extended polymerization times (20–27 minutes) further enhance coating integrity by increasing crosslinking density and allowing internal stress relaxation. Additionally, a 9-minute phosphating time improves surface activation and bonding, contributing to reduced crack formation.

5 CONCLUSION

The present study systematically investigated the effects of polymerization time, temperature, and phosphating time on the crack length of electrophoretic coatings applied to cold-rolled low-carbon steel, a material widely used in the automotive sector. Statistical analysis demonstrated that the model used to describe the variability in crack length was highly reliable, with an R² value of 0.75 and an adjusted R² of 0.70, indicating that a significant portion of the observed variability could be attributed to the chosen experimental parameters.

Graphical analysis showed that polymerization time and temperature significantly influenced crack length, with longer polymerization times generally resulting in larger cracks, especially at higher temperatures. A complex interaction between phosphating time and polymerization duration was also observed, with optimal crack length reductions occurring at specific time combinations for both factors. It was observed that under lower polymerization conditions, crack patterns were more irregular with broader spacing, which could be attributed to insufficient polymerization and thermal energy, leading to reduced cohesion and less uniformity in the coating. On the other hand, under higher polymerization conditions, a more uniform coating was achieved, with narrower and fewer cracks. However, despite the improved uniformity, prolonged polymerization times at elevated temperatures led to increased crack lengths due to the effects of thermal stresses and shrinkage, which exacerbated crack propagation.

The statistical model, with an R^2 value of 0.754 and an adjusted R^2 of 0.703, demonstrated a strong correlation between the experimental parameters and crack length. The model explained 70.31% of the observed variability, as confirmed by ANOVA results ($p < 0.0001$), validating its predictive capacity. The lack-of-fit analysis ($p = 0.5389$) further supported the model's adequacy, indicating that residual variance did not exceed within-group variance. A mean crack length of 70.17 mm was established as a benchmark for assessing coating integrity, with significant variations in crack lengths observed under different experimental conditions.

Considering additional variables, such as humidity and surface roughness, could further enhance the accuracy and predictive power of the model. While the current model focuses on key processing parameters—such as polymerization time, temperature, and phosphating duration—these additional factors could indeed influence the formation and propagation of cracks in the cathodic electrodeposited coatings. In future work, extending the model to include these factors will improve its robustness, allowing for a better understanding of their impact on coating performance. Incorporating humidity and surface roughness into the experimental design and statistical modeling will provide a more comprehensive approach to optimizing process conditions for enhanced coating quality and reduced crack formation.

ACKNOWLEDGMENTS

This work was funded by the Slovak Research and Development Agency under contract No. APVV- 20-0514. This work was supported by project VEGA 1/0391/22. This article is the result of the following project implementation: Development of excellent research capacities in the field of additive technologies for the Industry of the 21st century, ITMS: 313011BWN5, supported by the Operational Program Integrated Infrastructure funded by the ERDF.

REFERENCES

[Akafuah 2016] Akafuah, N.K. et al. Evolution of the Automotive Body Coating Process – A Review. Journal Coatings, 2016, Vol.6, No.2., 24. https://doi.org/10.3390/coatings6020024

[Almeida 2003] Almeida, E., et al. Cataphoretic and autophoretic automotive primers. A comparative study. Progress in Organic Coatings, 2003, Vol.46, pp 8-10. https://doi.org/10.1016/S0300-9440(02)00144-3

[Besra 2007] Besra, L. and Liu, M. A review on fundamentals and applications of electrophoretic deposition (EPD). Progress in Material Science, 2007, Vol.52, pp 1–6. ISSN 0079-6425. https://doi.org/10.1016/j.pmatsci.2006.07.001

[Brüggemann 2007] Brüggemann, M. and Rach, A. Electrocoat: Formulation and Technology. Hannover, Germany: Vincentz Network, 2020. ISBN 978-3-7486-0105-0.

[Calovi 2021] Calovi, M., et al. Synergic behavior of graphene-based filler and thermochromic pigments in cataphoretic coatings. Progress in Organic Coatings, 2021, Vol.150, 105978, ISSN 0300-9440. https://doi.org/10.1016/j.porgcoat.2020.105978

[Deflorian 2006] Deflorian, F., et al. Improvement of corrosion protection system for aluminium body bus used in public transportation. Materials & Design, 2006, Vol.27, pp 758–769, ISSN 0261-3069. https://doi.org/10.1016/j.matdes.2004.12.008

[Fejko 2024] Fejko, P., et al. Analysis of the effect of pretreatment on the overall damage of the coating created by the cataphoretic coating. MM Science Journal, October 2024, Vol. 5. https://doi.org/10.17973/MMSJ.2024_10_2024081

[Goeke 2014] Goeke, S., et al. Enhancing the Surface Integrity of Tribologically Stressed Contacting Surfaces by an Adjusted Surface Topography. In: 2nd CIRP Conference on Surface Integrity (CSI). Procedia CIRP, 2014. pp 214–218. https://doi.org/10.1016/j.procir.2014.04.037

[Grzesik 2016] Grzesik, W. Influence of Surface Textures Produced by Finishing Operations on their Functional Properties. Journal of Machine Engineering, February 2016. Vol.16, No.1., pp 15-23.

[Krasinskyi 2021] Krasinskyi, V., et al. Study of the structure and thermal characteristics of nanocomposites based on polyvinyl alcohol and intercalated montmorillonite. Journal of Thermoplastic Composite Materials, December 2021, Vol.34, No.12, pp 1680-1691. https://doi.org/10.1177/0892705719879199

[Olivier 2005] Olivier, M.G., et al. EIS evaluation of the filiform corrosion of aluminium coated by a cataphoretic paint. Progress in Organic Coatings, 2005, Vol.52, pp 263–270. https://doi.org/10.1016/j.porgcoat.2004.05.008

[Peti 2005] Peti, D., et al. The Effect of Degreasing Temperature on the Thickness of the Formed Layer Created by Cataphoretic Painting. MM Science Journal, November 2024, Vol.5. https://doi.org/10.17973/MMSJ.2024_11_2024085

[Romano 2006] Romano, A.P., et al. Influence of the curing temperature of a cataphoretic coating on the development of filiform corrosion of aluminium. Progress in Organic

Coatings, 2006, Vol.57, pp 400–407. https://doi.org/10.1016/j.porgcoat.2006.09.024

[Rossi 2006] Rossi, S. et al. Corrosion protection of aluminium foams by cataphoretic deposition of organic coatings. Journal Progress in Organic Coatings, 2017, Vol.109, pp 144-151. https://doi.org/10.1016/j.porgcoat.2017.04.042

[Skotnicki 2021] Skotnicki, W. and Jedrzejczyk, D. The Comparative Analysis of the Coatings Deposited on the Automotive Parts by the Cataphoresis Method. Journal Materials, October 2021, Vol.14, No.20., 6155. https://doi.org/10.3390/ma14206155

[Sternadelova 2023] Sternadelova, K., et al. Quality assessment of the vitreous enamel coating applied to the weld joint. MM science Journal, March 2023, Vol. 1. https://doi.org/10.17973/MMSJ.2023_03_2022105

[Trzepiecinski 2023] Trzepiecinski, T., et al. Friction Behaviour of 6082-T6 Aluminium Alloy Sheets in a Strip Draw Tribological Test. Materials, March 2023, Vol.16, No.6. https://doi.org/10.3390/ma16062338

[Zanella 2014] Zanella, C., et al. Influence of the electrochemical behavior of metal substrates on the properties of cataphoretic clearcoat. Progress in Organic Coatings, 2014, Vol.77, pp 1987-1992. https://doi.org/10.1016/j.porgcoat.2014.06.019

CONTACTS:

Damian Peti, MSc.
Technical University of Kosice, Faculty of Manufacturing Technologies with a seat in Presov
Bayerova 1, Presov, 08001, Slovakia
+421917554828, damian.peti@tuke.sk, fvt.tuke.sk